Comparative Study and Qualitative-Quantitative Investigations of Several Motion Deblurring Algorithms

Ashwini M. Deshpande
Department of Electronics Engineering
S. V. National Institute of Technology, Surat, India

Suprava Patnaik
Department of Electronics Engineering
S. V. National Institute of Technology, Surat, India

ABSTRACT
Motion blur caused by relative motion between the camera and the object being captured is an everyday situation that deteriorates the quality of the images largely. Even a photograph captured in low light conditions or that of a fast moving object undergo motion blur and cause significant degradation of the image and demands for deblurring the same to reconstruct the original image. The paper addresses this commonly encountered problem and carries out a thorough experimental investigation of several non-blind and blind motion deblurring algorithms. Both qualitative and quantitative assessment based on popular performance metrics viz., peak signal-to-noise ratio (PSNR) and mean squared error (MSE) is performed. Through this comparative analysis the properties and limitations of these deblurring algorithms are explored and verified.

General Terms
Algorithms, Performance, Experimentation.

Keywords
Deblurring, Deconvolution, Motion blur, Point Spread function, Gaussian noise.

1. INTRODUCTION
Image motion deblurring, although being a traditional problem in image processing, is still a challenging area and has always attracted the attention of both research community and photographic practitioners equally till date. A number of real world problems from astronomy, medical imaging up to consumer level photography demands a good quality image for number of reasons, viz., object detection, identification or classification. Thus, there is undying need for removing motion blur (due to any reason), by means of image deblurring algorithms [1]. There also exist compensation mechanisms to prevent this effect to occur, such as gyroscope and inertial sensors in case of aerial sensing, moving lens systems or optical image stabilization systems in the case of digital cameras [2, 15]. These solutions partially remove the blur at the expense of higher cost, weight and energy consumption. The rapidly growing field of digital photography demands on more and more improvements in image quality at lower costs and computationally faster post-processing solutions by virtue of recent advances in image processing.

The overall approach comprises of taking a standard (non-blurred) image, creating a known blurring function (point spread function-PSF) and then filtering the image with this function so as to add blur into it. This image is further corrupted by different amount of additive Gaussian noise. The aim is to deblur this image by various motion deblurring algorithms viz., direct inverse and pseudo-inverse filtering, Wiener and parametric Wiener filtering, constrained least squares filtering, Richardson-Lucy algorithm and iterative blind deconvolution algorithm. Further their properties and performances are analyzed and compared as well. Experimental evaluation is carried out in MATLAB environment on standard lena and cameraman images in a variety of blur and noise conditions.

The rest of the paper is arranged as follows. The mathematical modeling of linear motion blur is discussed in Section 2. An overview of the important deblurring algorithms and their detail characteristics are presented in Section 3. A complete experimental set-up is described in Section 4. Section 5 comprises of both qualitative and quantitative results obtained based on the experiments conducted and performance evaluation of the deblurring algorithms discussed in earlier section. Conclusions are drawn in Section 6 and Section 7 briefs the future scope for further improving the existing algorithms and challenges in doing so.

2. MODELING LINEAR MOTION BLUR
A linear mathematical model is used to represent the degradation of the digital image caused by motion blur [1, 9]. The original test image is considered to be a blur-free $M \times N$ test image f which is convolved with a convolution kernel h, also referred to as the point spread function (PSF). In the spatial domain, the distortion operator, i.e., the PSF describes the degree to which an optical system blurs (spreads) a point of light. It is due to the capture process where some noise gets introduced, which is modeled with the additive Gaussian noise term n. Thus, the blurred and noisy $M \times N$ image g, is modeled as,

$$g(x,y) = f(x,y) \otimes h(x,y) + n(x,y) = \int_{-\infty}^{\infty}\int_{-\infty}^{\infty} f(r,c)\, h(x-r, y-c)\, dr\, dc + n(x,y), \quad (1)$$

where h is a linear PSF, f is the ideal image and g is the observed image. It is considered that the type of blur is spatially invariant i.e., the blur is independent of position or a blurred object looks the same irrespective of its position in the image. In this case and for the uniform linear motion, the PSF $h(x,y)$ is given by:

$$h(x,y;L,\varphi) = \frac{1}{L} \quad if \ \sqrt{x^2+y^2} \le \frac{L}{2} \quad and \ \frac{x}{y} = -\tan\varphi \quad (2)$$
$$= 0 \quad elsewhere$$

As seen in Eq. (2), motion blur depends on two parameters: motion length (L) and motion direction (φ). The problem of identifying these parameters from the motion blurred scene is termed as PSF estimation [4]. The process of motion deblurring

can be divided into two parts: the estimation of the function that caused the blur, and applying a deblurring algorithm. Based on the assumption of a generalized Gaussian model for the additive noise, this paper discusses only about applying deblurring algorithms to the motion blurred images, whereas for the first part i.e., the PSF model for motion blur is assumed to be known. Deconvolution results may deviate from the actual images because of presence of noise and low pass filtering effect in original image.

3. CLASSICAL DECONVOLUTION METHODS

The classical deconvolution algorithms perform deblurring operation on the already blurred and noise corrupted image g and produces an estimate $\hat{f}$ of the undegraded image f. The non-blind methods which are discussed here are namely, inverse and pseudo-inverse filter, Wiener and parametric-Wiener filter; constrained least squares filter (CLS), Richardson-Lucy (R-L) algorithm [5], where it is assumed that the characteristics of the degrading system and the noise are known a priori. Another class which is based on real life fact that such information about degrading system at the time of image formation is rarely available is blind deconvolution. One of the methods of this class is the iterative blind deconvolution (IBD), it is also described in detail. A large class of inverse problems uses these algorithms based on the available information about the blurring phenomenon in a specific application [18].

3.1 Direct Inverse Filtering

If a good model of the blurring function that corrupted an image is known or can be developed, then inverse filtering is the quickest and easiest way to restore the blurred image. Since blurring is equivalent to low pass filtering of an image, inverse filtering provides with high pass filtering action to reconstruct the blurred image without much effort. Figure 1 depicts complete blurring and deblurring operation that the image undergoes in case of direct inverse filtering.

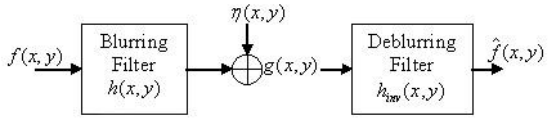

Fig 1: A block diagram representation of direct inverse filter.

The notations used are, g is the blurred and noise corrupted image, $\hat{f}$ is the estimate of the undegraded image f, the additive Gaussian noise is denoted as η. Referring Eq. (1), convolution can be alternatively implemented through the use of the frequency domain, which yields

$$G(u,v) = H(u,v) \cdot F(u,v) + N(u,v) \tag{3}$$

where (u,v) are the spatial frequency coordinates and capitals represent Fourier transforms. When the additive noise is unknown, it is assumed to be zero. Rewriting Eq. (3), the spectral representation of estimated image can be directly obtained from the following relationship:

$$\hat{F}(u,v) = \frac{G(u,v)}{H(u,v)} \tag{4}$$

This gives us direct filtering requiring only the blur PSF as *a priori* knowledge, and it allows for perfect restoration in the case that noise is absent. Unfortunately, since the inverse filter is a form of high pass filer, inverse filtering responds very badly to any noise that is present in the image because noise tends to be high frequency. Although there are some schemes to improve the performance of inverse filter viz., thresholding and iterative methods; they tries to tackle the noise term for limiting the amplification of it, but there lies trade-off between deblurring and denoising. A thresholding scheme that handles the smaller or near zero values of inverse filter is *pseudo-inverse filtering*. So instead of making a full inverse out of H (i.e., high pass filter), it is modified to become 'less' full inverse as follows,

$$H_{inv}(u,v) = \begin{cases} \dfrac{1}{H(u,v)} & for \quad |H(u,v)| > \delta \\ 0 & for \quad |H(u,v)| \leq \delta \end{cases} \tag{5}$$

So the higher the value of δ, the closer H_{inv} is towards the full inverse filter. It can be selected in the range of $0 \leq \delta \leq 1$. The smaller the δ, the less high pass the filter is, which means that it amplifies noise less. It also means, however, that the edges will not be as sharp as they could be, but it performs better than direct inverse method.

3.2 Wiener Filter

The Wiener filter [5] also termed as seeks to minimize the following error function,

$$MSE = E\left[\left| f(x,y) - \hat{f}(x,y) \right|^2 \right] \tag{6}$$

where $E[.]$ denotes the expected value operator, $f(x,y)$ and $\hat{f}(x,y)$ stands for original and estimated image respectively. The solution to this optimization task in the frequency domain can be written as follows,

$$H_{wiener}(u,v) = \frac{H^*(u,v)}{H^*(u,v)H(u,v) + \dfrac{S_n(u,v)}{S_f(u,v)}} \tag{7}$$

where $H^*(u,v)$ is the complex conjugate of $H(u,v)$, $S_f(u,v)$ and $S_n(u,v)$ are the power spectrum of the ideal image and the noise, respectively. The power spectrum is a measure for the average signal power per spatial frequency (u,v) carried by the image. In the noiseless case $S_n(u,v) = 0$, thus the Wiener filter approximates the inverse filter. When the recorded image is noisy, the Wiener filter trades-off the restoration by inverse filtering and suppression of noise for those frequencies where $H(u,v)$ is closer to 0. The important factors in this trade-off are the power spectra of the ideal image and the noise. The ratio of $S_n(u,v)$ and $S_f(u,v)$ in Eq. (7) is termed as noise-to-signal ratio (NSR). Wiener filter requires the power spectra of noise and image to be known. When they are not known the ratio is approximated by user and is determined by trial and error such as to minimize the error function. The

form obtained in Eq. (8) is thus termed as *parametric-Wiener filter*.

$$H_{wiener}(u,v) = \frac{H^*(u,v)}{\left|H(u,v)\right|^2 + K} \tag{8}$$

where K has a small positive value and is usually selected in the range of $0 < K < 1$ so as to minimize the error function. Wiener performs better than direct inverse method in presence of noise, but subject to a priori knowledge about blurring function, the image and noise power spectrums and/or appropriate selection of K. Even better results than the known power spectra method can be achieved using the known autocorrelations of the original image and the noise. As the autocorrelation of noise could in many cases be considered relatively constant over time, a high pass filtering of the autocorrelation sequence, could lead to substantial reduction of the noise effect.

3.3 Constrained Least Squares Filter

The constrained least-squares filter (CLS) [6, 5] is another approach for overcoming some of the difficulties of the inverse filter (excessive noise amplification) and of the Wiener filters (estimation of the power spectrum of the ideal image), while still retaining the simplicity of a spatially invariant linear filter. But it is required to have a priori knowledge about mean and variance of the noise. The CLS algorithm is based on finding a direct solution using a criterion C, which ensures optimal smoothness of the deblurred image. It provides more reasonable expectation for the restored image that it satisfies

$$\left\| g - h \otimes \hat{f} \right\|^2 = \left\| \eta^2 \right\| \tag{9}$$

Thus the filter reconstruction task is to find the minimum of

$$C = \sum_{k_1=0}^{N-1} \sum_{k_2=0}^{M-1} \left[\nabla^2 f(k_1, k_2) \right]^2 \tag{10}$$

under the constraint of Eq. (9). In the frequency domain the solution to this problem can be written as follows:

$$H_{cls}(u,v) = \frac{H^*(u,v)}{H^*(u,v)H(u,v) + \alpha P^*(u,v)P(u,v)} \tag{11}$$

where α is the parameter which has to be adjusted manually or iteratively, to fulfill the constraint C and $P(u,v)$ is the Laplacian operator in the frequency domain. Choosing the value of the regularization parameter α is a critical issue in regularized restoration, since it controls the trade-off between fidelity to the data and smoothness of the solution and therefore the quality of the restored image. A number of approaches for determining its value are presented and compared in [8, 13].

3.4 Richardson-Lucy Algorithm

The Richardson-Lucy (R-L) algorithm can be viewed as a maximum-likelihood (ML) method for image deblurring when the data noise is assumed to be Poissonian. This iterative method was developed independently by Richardson and Lucy [10, 7], is the technique most widely used for deblurring and restoration of images. Since R-L exploits the *a priori* knowledge regarding the statistics of photon counts, it should be expected to yield more accurate reconstructions than an approach that does not use this information. The algorithm works with images blurred by a valid point spread function. Also, the restored images are robust against small errors in the point spread function, which is very important when the PSF is not known exactly and only estimation is available. The R-L algorithm is well described in [11]. The R-L method forces the restored image to be non-negative. Given that the degraded image and the first guess are everywhere non-negative, none of further approximations can be negative. The steps of the algorithm are summarized below:

The algorithm consists of one initial and three iterative steps. Initially the first approximation of the restored image $\hat{f}_0$ must be made, which is typically the constant average of all pixel values in the blurred image g. In the iterative steps, further, the $(n+1)^{th}$ estimate of the restored image is given by the n^{th} estimate of the restored image multiplied by a correction image i.e.,

$$\hat{f}_{n+1} = \hat{f}_n \cdot \varphi_n \tag{12}$$

where $\hat{f}_{n+1}$ is the new and $\hat{f}_n$ is the current approximation of restored image respectively, φ_n is known as the correction factor and $\cdot$ denotes a "pixel-by-pixel" multiplication. The correction factor is computed as,

$$\varphi_n = \overleftarrow{h} \otimes \frac{g}{h \otimes \hat{f}_n} \tag{13}$$

where $\overleftarrow{h}$ denotes the PSF in reverse order. The algorithm continues with step 2 until the corrections are sufficiently small. While using this method, there arises an obvious question of where to stop. It is difficult to claim any specific value for the number of iterations; a good solution depends on the size and complexity of the PSF matrix. The algorithm usually reaches a stable solution very quickly (few steps) with a small PSF matrix. But if one stops after a very few iterations then the image may be very smooth. On the other hand, increasing the number of iterations not only slows down the computational process, but also amplifies noise and introduces the *ringing effect* (as shown in Figure 9). Proper boundary condition selection and/or using the built-in edge tapering function in Matlab tries to reduce these ringing artifacts. Some additional methods for ringing reduction are given in [3]. Thus for the "good" quality of restored image, the optimal number of iterations are determined manually for every image as per the PSF size.

3.5 Iterative Blind-deconvolution Algorithm

The techniques discussed so far belongs to the class of classical image restoration or deblurring, where blurring function is known and the degradation process is inverted using one of the many known deblurring algorithms. The selection of the particular algorithm depends upon mathematical model of both the degradation process and image. On the other hand, blind image deblurring handles more difficult, but realistic problem where the amount of blur or degradation is not known and little information is available about the original image; thus previous algorithms are not suitable as they all require prior knowledge of the PSF that was used to blur it. In these situations, an algorithmic approach that combines blur identification and image deblurring both is required. Such an estimation problem,

assuming the linear degradation model, is termed as *blind image deconvolution (BID)* [14, 18], where the image $f(x; y)$ must be identified directly from the convolved signal $g(x; y)$ using partial or no information about the blurring process and true image. Thus, BID is the process of estimating both the true image and the blur from the degraded image characteristics using partial information about the imaging system. BID problem is classified into two categories depending on at what stage the blur is being identified i.e., *a priori* or jointly with the image [4, 16]:

One of the popular blind deconvolution algorithms is the iterative blind deconvolution (IBD) algorithm proposed by [12]. The IBD algorithm iteratively estimates the original image as well as the PSF. IBD makes use of spatial domain as well as frequency domain constraints. In spatial domain, positivity constraint is used on both the image as well as PSF. Positivity is used in spatial domain because image pixel intensity values are always positive. Similarly, PSF values are observed to be always positive. The Fourier domain constraint may be described as constraining the product of the Fourier spectra of $f(x; y)$ and $h(x; y)$ to be equal to the Fourier spectra of $g(x; y)$, as followed in Eq. (14).

$$G(u,v) = F(u,v)H(u,v) \tag{14}$$

3.5.1 IBD Algorithm

1. Estimate a non-negative-valued initial PSF $h(x, y)$ with random values.
2. Find $\hat{H}_k(u,v)$ by taking discrete Fourier transform (DFT) of $h_k(x, y)$.
3. Compute $F_k(u,v)$ i.e. the first estimate of the original image spectrum from $G(u,v)$ and $\hat{H}_k(u,v)$, as $F_k(u,v) = \dfrac{G(u,v)}{\hat{H}_k(u,v)}$.
4. Compute the inverse Fourier transform (IDFT) of $F_k(u,v)$, to obtain $f_k(x, y)$.
5. Impose the spatial domain constraint of positivity by putting zero to all pixels of $f_k(x, y)$ that have a negative value.
6. Obtain $\hat{F}_k(u,v)$ after Fourier transforming a positive constrained estimate $\hat{f}_k(x, y)$.
7. Compute $H_k(u,v)$, from $G(u,v)$ and $\hat{F}_k(u,v)$, as $H_k(u,v) = \dfrac{G(u,v)}{\hat{F}_k(u,v)}$.
8. Compute the IDFT of the next spectrum estimate $H_k(u,v)$, to obtain $h_k(x, y)$.
9. Impose the positivity constraints on $h_k(x, y)$, that yields the next PSF estimate.

The iterative loop is repeated until a satisfactory restored image is obtained. Although the calculations involved here are quite straightforward and appealing, the output is not definite, the algorithm may run into infinite loop without converging and it is quite sensitive to the initial guess [13, 14].

4. EXPERIMENTAL SET-UP

The experiments of motion blurring and deblurring the images are carried out in Matlab 7.0.1. The experimentation set-up is as follows,

- **Parameter selection scheme**:
  - Test images: lena and cameraman
  - Type of blur: Motion Blur (Attributes-Length= 10 pixels, Angle= 45 degrees)
  - Type of noise: Additive Gaussian with mean=0, standard deviation=1, 10, 20, 30, 40, 50
- **Deblurring techniques**:
  - Direct Inverse filtering
  - Pseudo Inverse filtering ($\delta = 0.1$)
  - Wiener filter by known image and noise power spectrums and by known autocorrelations of image and noise
  - Parametric Wiener ($K = 0.1, 0.001, 0.0001$)
  - Constrained Least Squares (CLS) method ($\alpha = 0.4, 0.04, 0.004, 0.1$)
  - Richardson-Lucy Algorithm (Poisson noise with var.= 0.002, 0.0001 and PSF size= 5×5 and 9×9)
  - Iterative blind deconvolution.
- **Evaluation metrics**: MSE and PSNR.

To assess the performance of the different deblurring methods and to evaluate their comparative performance, two different standard performance indices have been used in this paper. They are namely Peak Signal to Noise Ratio (PSNR) and Mean Squared Error (MSE) and are defined as:

$$PSNR(dB) = 10\log_{10}\left(\frac{255^2}{MSE}\right) \tag{15}$$

$$MSE = \frac{1}{MN}\sum_{x=1}^{M}\sum_{y=1}^{N}\left[f(x,y) - \hat{f}(x,y)\right]^2 \tag{16}$$

where MN is the size of the image, $f(x,y)$ and $\hat{f}(x,y)$ are the pixel values at $(x,y)^{th}$ location of original and restored image respectively. The higher the PSNR and lower the MSE in the deblurred image, the better is its quality. These metrics serve to provide an objective standard to compare different techniques. Moreover human perception is the visual key indicator of improvement in quality for subjective comparisons of various deblurring algorithms.

5. PERFORMANCE EVALUATION

5.1 Direct Inverse Filtering

Figure 2 shows the results obtained with direct inverse filtering method. The only-motion blurred cameraman image without noise is successfully restored in this method.

Fig 2: Results obtained using direct inverse filtering (a) Original image, (b) Blurred image, (c) Inverse filtered image.

5.2 Inverse and Pseudo-inverse Filtering

Now noise is added in the earlier blurred image and is filtered by two ways- by direct inverse filtering and pseudo-inverse filtering. As seen in the resulting Figure 3, in the direct inverse filter, noise completely overshadows the underlying image, whereas the pseudo-inverse filtering ($\delta = 0.1$) attempts to give better quality result than the former method.

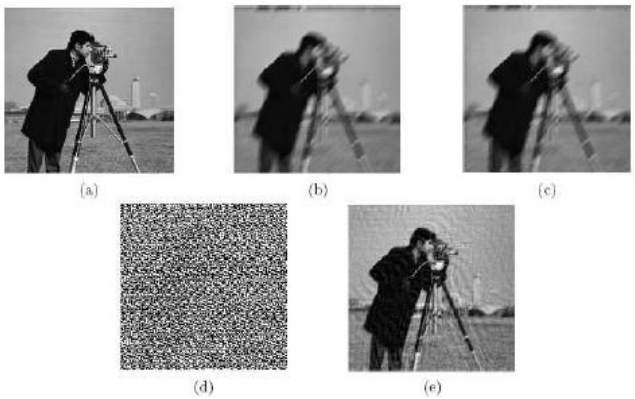

Fig 3: Results obtained using inverse and pseudo-inverse filtering (a) Original image, (b) Blurred image, (c) Blurred and noisy image (d) Inverse filtered image (e) Pseudo-inverse filtered image.

5.3 Wiener Filtering

Figure 4 presents plot of PSNR versus standard deviation comparison for original blurred image and Wiener filtered image by known power spectra and autocorrelation methods. As seen below the autocorrelation method gives more PSNR than the power spectra method. Similarly, both the methods are compared for the resulting MSE of the restored images and original MSE for varying the standard deviation in Figure 5. It shows that the autocorrelation method gives least MSE than the power spectra method and original one.

5.4 Parametric Wiener Filtering

When the power spectra or autocorrelation can not be determined directly, the parametric Wiener filter is used. In this method the noise-to-signal power ratio is approximated by the factor K , which is substituted by trial and error as a small positive value. Figure 6 shows the results by parametric Wiener filtering for blurred noisy image with BSNR of 20dB; for three different values of K i.e., for K = 0.1, 0.01 and 0.001. Figure 7 depicts the plot of PSNR versus standard deviation for original blurred image and parametric Wiener filtered image for three different values of K . It can be seen that PSNR is more for smaller values of K , as the image becomes sharper but the noise

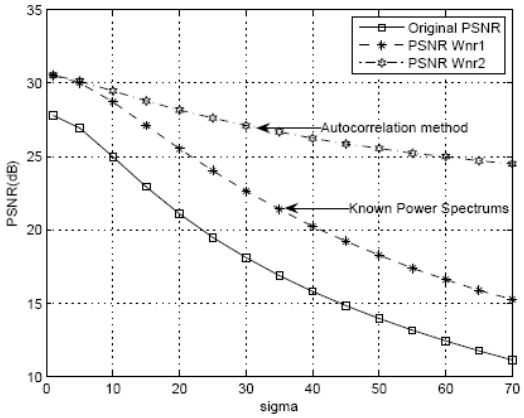

Fig 4: A plot of PSNR versus standard deviation for original blurred image and Wiener filtered image by known power spectra and autocorrelation methods.

amplification problem which becomes more noticeable, trades off the selection of this value over the larger values of K , for which noise is suppressed but edges are blunt due to smoothness.

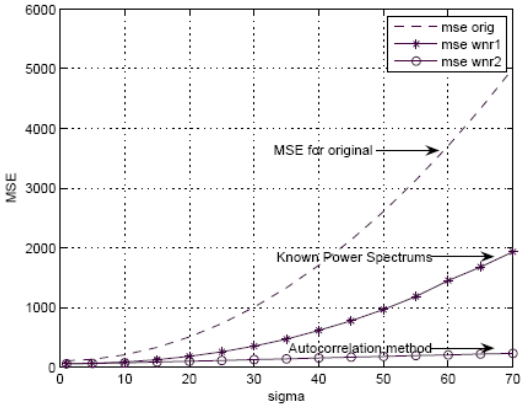

Fig 5: A plot of MSE versus standard deviation for original blurred image and Wiener filtered image by known power spectra and autocorrelation methods.

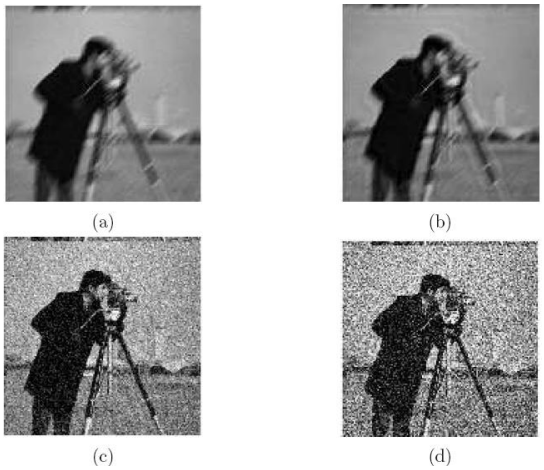

Fig 6: Results obtained using parametric Wiener filtering with different values of K (a) Blurred and noisy image with BSNR=20 dB, (b) K = 0.1, (c) K = 0.01 (d) K =0.001.

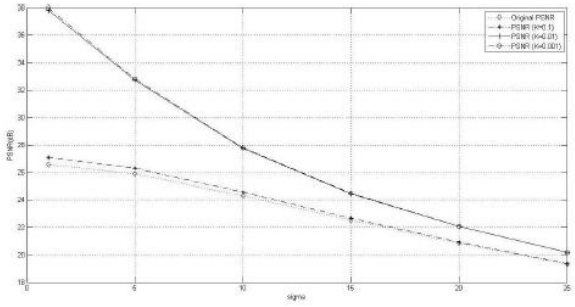

Fig 7: A plot of PSNR versus standard deviation for original blurred image and parametric Wiener filtered image for three different values of *K*.

5.5 Constrained least-squares method

The plot of PSNR versus standard deviation for original blurred image and constrained least squares filtered images for different values of α in Figure 9 and that of MSE versus standard deviation in Figure 8 shows optimal performance (larger PSNR and smaller MSE) for smaller value of $\alpha = 0.004$. At this value, although edges are sharpened but the problem of ringing becomes prominent.

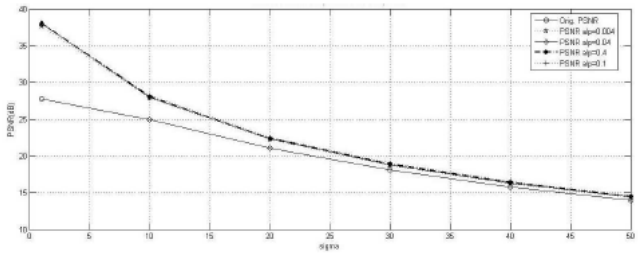

Fig 8: A plot of PSNR versus standard deviation for original blurred image and constrained least squares filtered image for different values of α .

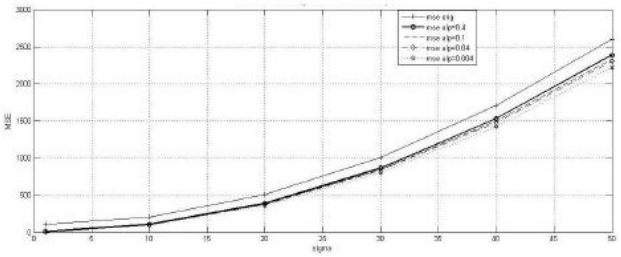

Fig 9: A plot of MSE versus standard deviation for original blurred image and constrained least squares filtered image for different values of α .

5.6 Richardson-Lucy Algorithm

The results of deblurred image by iterative Richardson-Lucy (R-L) algorithm based upon Poisson noise statistics are collectively presented in Figure 10 for the originally motion blurred and noise corrupted (Poissonian noise with variance= 0.002) image. As the numbers of iterations of R-L algorithm are increased, the ringing artifacts become prominent in the deblurred images, along with increased amount of execution time. Thus, this method is slower as compared to previous methods of deblurring.

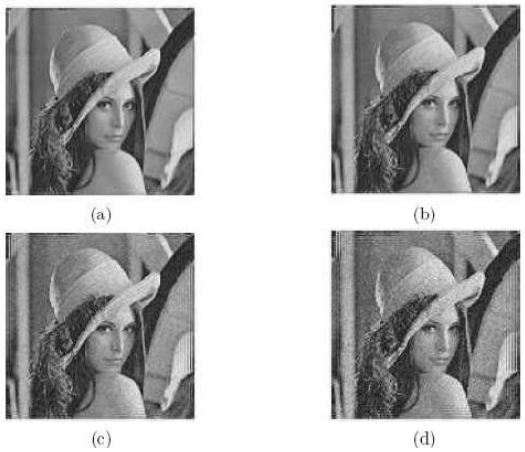

Fig 10: Results obtained using Richardson-Lucy algorithm with number of iterations equal to (a) 10, (b) 15, (c) 25 and (d) 35.

Figure 11 and 12 show the plots of PSNR versus number of iterations for two different sizes of PSF i.e., 5×5 and 9×9 and for two different noisy conditions i.e., variances= 0.002 and 0.0001. PSNR is better for 9×9 i.e., large PSF size and it is lowered in case of more noise even though PSF size is large. Too large sizes of PSF distort the image quality largely, increases the execution time and strong deconvolution artifacts incorporates if number of iterations are more than 50. Thus, it is critical to select the PSF size and number of iterations for successful deblurring for limited knowledge about PSF.

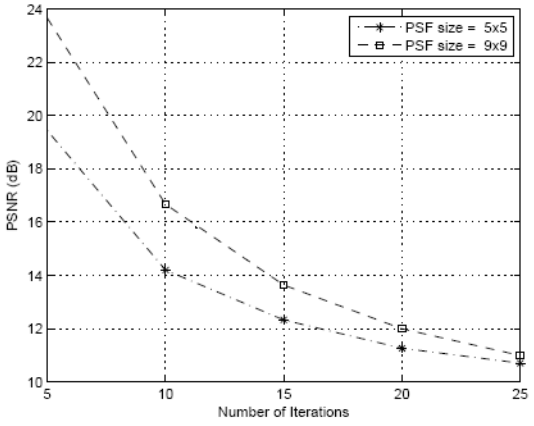

Fig 11: A plot of PSNR versus number of iterations for two different sizes of PSF i.e., 5×5 and 9×9 for variance= 0.002.

5.7 Iterative Blind-deconvolution Algorithm

Inputs to the IBD algorithm are original blurred image, an initial guess of the PSF and the number of iterations. It follows same mathematical process as Richardson-Lucy, except it can be used without knowledge of PSF and restores the image as well as PSF [16, 17]. While implementing the IBD algorithm in Matlab, it is applied on the motion blurred cameraman image in two different ways [5]:

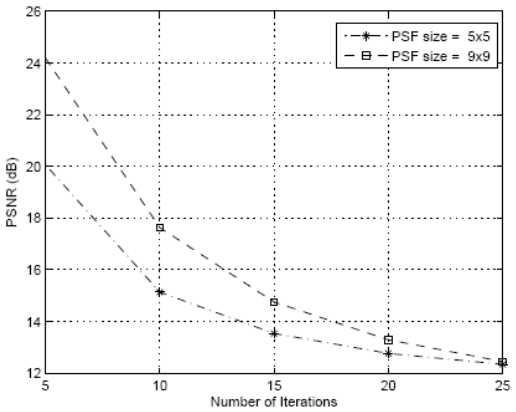

Fig 12: A plot of PSNR versus number of iterations for two different sizes of PSF i.e., 5×5 and 9×9 for variance= 0.0001.

I. It generates an initial PSF of chosen values of the motion attributes of the blur and then gets the size of that PSF for the initial PSF guess, but with all elements set to one.
II. The size of the PSF is simply guessed with all elements set equal to one or the matrix size of the desired PSF can simply be specified and the algorithm iterates to find the best values.

Figure 13 shows the results obtained using IBD algorithm for these two cases. As verified experimentally, if the initial guess of the PSF is the same size as the PSF that caused the blur (method I), lot of ringing artifacts are observed around the sharp intensity contrast areas in the deblurred image as shown in Figure (13-d).

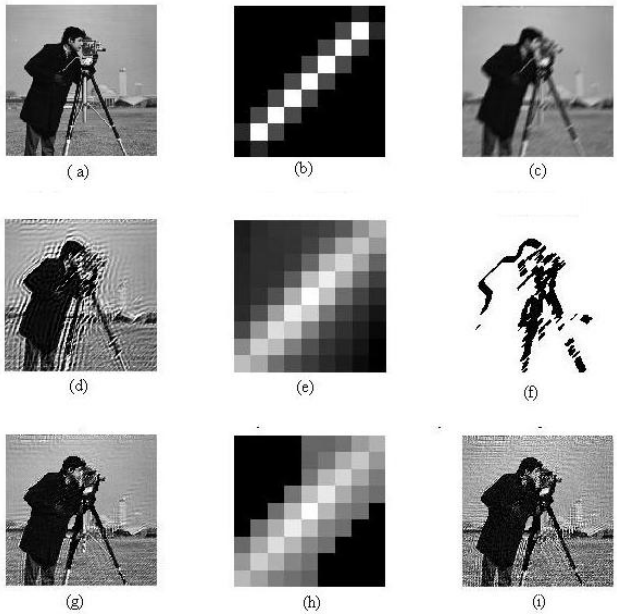

Fig 13: Results obtained using iterative blind deconvolution algorithm (a) Original image, (b) Original PSF, (c) Blurred image, (d) Restored image with case (1), (e) Restored PSF for case (1), (f) Weight array, (g)-(h) Newly deblurred image and Restored PSF after 50 iterations for case (2), (i) Newly deblurred image after 150 iterations for case (2).

To minimize the ringing effect, a weight array is created to exclude areas of high contrast from the deblurring operation. Further, to improve the deblurring, the PSF guess is refined according to method II and IBD algorithm is iterated for different number of iterations and various sizes of PSF until satisfactory deblurred image is resulted. Figure (13-e and h) displays the restored PSF, observation of which helps refining the new PSF size.

Figure 14 and 15 reflects the quantitative measure for the IBD algorithm. As shown in the plots, PSNR level goes on decreasing and MSE curves goes on increasing for increase in size of PSFs, which is the indication of lowering the quality of deblurred image. Also it implies that the convergence of the algorithm is not well defined and is subject to the perception of the quality of results either at the end of every iteration or after few number of iterations. Histogram plot in Figure 16 accounts for the processing or computation time required to run IBD for the specified number of iterations. Although for increasing number of iterations increases the computational time, it doesn't always show improvement in the quality of deblurring for large number of iterations. It was found that for the iterations above 200, the amount of ringing and deblurring is remaining almost same. So there is no point in further increasing the number of iterations.

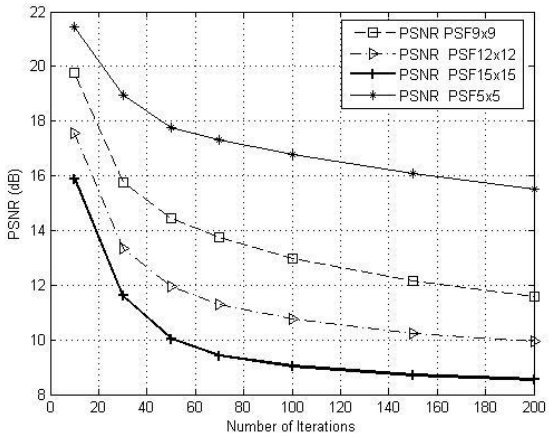

Fig 14: A plot of PSNR versus number of iterations for different sizes of PSF for IBD.

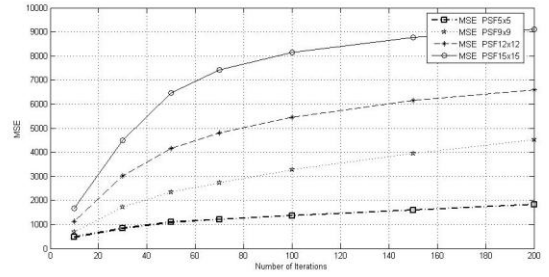

Fig 15: A plot of MSE versus number of iterations for different sizes of PSF for IBD.

6. CONCLUSIONS

In this paper, the performances of the basic deblurring techniques are studied and compared only for synthetically blurred images. The most simple algorithm direct inverse

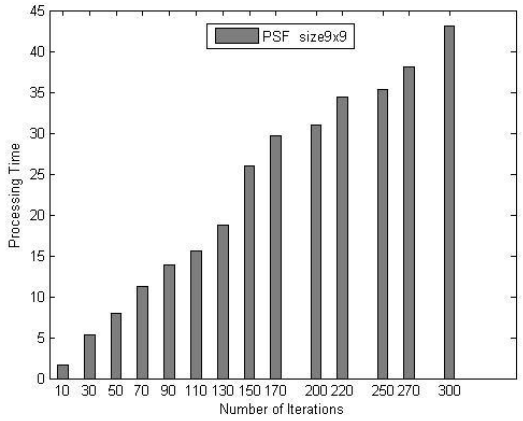

Fig 16: Processing time versus number of iterations for IBD.

filtering fails completely in presence of noise, as the noise is amplified badly. Both the Wiener and constrained least squares algorithms show comparable results, which comprise a lot of low frequency ringing, but restore the contours more or less satisfactorily. The deblurred images by these two methods show acceptable results in low noise conditions. But again noise quality in deblurred image is subject to the amount of noise, extent of blur and choosing the appropriate regularization term. As the Richardson-Lucy algorithm is derived from counting statistics by means of maximizing the likelihood of the solution, it restores the seriously blurred and noisy image in real life better than the former two methods and outperforms. In the IBD method, the majority of the blur is successfully removed, but ringing effect could be seen across the entire image and some of the details of the image are getting washed away. Thus, in the blind deconvolution, it is possible to restore blurred image based upon correct PSF estimation and sufficient *a priori* knowledge about the image and noise.

7. FUTURE SCOPE

Motion deblurring work can be further extended on real images, where lot of other aspects including retaining color information and effective noise suppression need additional concern along with basic deblurring. It will be interesting to note how Wiener and CLS perform if effective denoising is performed earlier and then these methods are applied for deblurring. In case of R-L and IBD, longer run time, ringing artifacts and appropriate termination criteria for the iterations are the important issues, where further improvements need attention. IBD particularly tackles the harder and realistic problem, which becomes more complex for spatially varying object motion and recovery of original image from such type of blurs with no knowledge of PSF leaves a scope for developing more robust algorithms.

8. REFERENCES

[1] Banham, M. R. and Katsaggelos, A. K. Digital image restoration. IEEE signal processing magazine, 24-41, 1997.

[2] Ben-Ezra, M. and Nayar, S. K. Motion-based motion deblurring. IEEE Transactions on Pattern Analysis and Machine Intelligence, vol. 26, no. 6, 689-698, 2004.

[3] Bertero, M. and Boccacci, P. A simple method for the reduction of boundary effects in the Richardson-Lucy approach to image deconvolution. Astronomy and Astrophysics, 369-374, 2005.

[4] Chalmond, B. 1991. PSF estimation for image deblurring. CVGIP: Graphical Models and Image Processing, vol. 53, no. 4, 364-372.

[5] Gonzalez, R., Woods, R., and Eddins, S. Digital Image Processing Using MATLAB. Pearson Prentice-Hall, Upper Saddle River, NJ, 2004.

[6] Hunt, B. The application of constrained least squares estimation to image restoration by digital computer. IEEE Transactions on Computer, vol. 2, 805-812, 1973.

[7] Lucy, L. An iterative technique for the rectification of observed distributions. The Astronomical Journal, vol. 79, no. 6, 745-754, 1974.

[8] Mesarovic, V. Z., Galatsanos, N. P., and Katsaggelos, A. K. Regularized constrained total least squares image restoration. IEEE Transactions on Signal Processing, vol. 4, no. 8, 1096-1108, 1995.

[9] Moghaddam, M. E., and Jamzad, M. Motion blur identification in noisy images using mathematical models and statistical measures. Pattern Recognition, vol. 40, 1946-1957, 2007.

[10] Richardson, W. H. Bayesian-based iterative method of image restoration. Journal of the Optical Society of America, vol. 62, no. 1, 55-59, 1972.

[11] Jiang, X., Cheng, D. C., Wachenfeld, S., Rothaus, K. Motion Deblurring. University of Muenster, Department of Mathematics and Computer Science, 2005.

[12] Ayers G. R., and Dainty J. C. Iterative blind deconvolution methods and its applications. Optics Letter, vol. 13, no. 7, July 1988.

[13] Lajendijk, R. L., Biemond J., and Boekee, D. E. Regularized Iterative Image Restoration with Ringing Reduction. IEEE Transactions on Acoustics, Speech, and Signal Processing, vol. 36, no. 12, 1874-1888, 1988.

[14] Kundur D. and Hatzinakos D. A novel blind deconvolution scheme for image restoration using recursive filtering, IEEE Transactions on Signal Processing, vol. 46, no. 2, pp. 375-390, 1998.

[15] Raskar R., Agrawal A., and Tumblin J. Coded exposure photography: motion deblurring using fluttered shutter, ACM Transactions on Graphics (TOG), vol. 25, no. 3, 795–804, 2006.

[16] Biemond, J., Lagendijk, R., and Mersereau, R. M. Iterative methods for image deblurring," in Proceedings of the IEEE, vol. 78, no. 5, pp. 856-883, 1990.

[17] Shao-jie, S., Qiong, W., and Guo-hui, L. Blind image deconvolution for single motion-blurred image, The Journal of China Universities of Posts and Telecommunications, vol. 17, no. 3, pp. 104-109, 2010.

[18] Mariana, S. C., and Almeida, L. B. Blind and semi-blind deblurring of natural images, IEEE Transactions on Image Processing, vol. 19, no. 1, pp. 36-52, 2010.